Available online at www.sciencedirect.com
ScienceDirect
Trans. Nonferrous Met. Soc. China 22(2012) 1423−1431
Transactions of Nonferrous Metals Society of China
www.tnmsc.cn

Effects of high-energy ball milling oxide-doped and varistor ceramic powder on ZnO varistor

XU Dong[1,2,3], TANG Dong-mei[1,4], JIAO Lei[1], YUAN Hong-ming[5], ZHAO Guo-ping[1], CHENG Xiao-nong[1,4]

1. School of Materials Science and Engineering, Jiangsu University, Zhenjiang 212013, China;
2. Key Laboratory of Semiconductor Materials Science, Institute of Semiconductors, Chinese Academy of Sciences, Beijing 100083, China;
3. State Key Laboratory of Electrical Insulation and Power Equipment, Xi'an Jiaotong University, Xi'an 710049, China;
4. Changzhou Engineering Research Institute of Jiangsu University, Changzhou 213000, China;
5. State Key Laboratory of Inorganic Synthesis and Preparative Chemistry, College of Chemistry, Jilin University, Changchun 130012, China

Received 31 May 2011; accepted 15 February 2012

Abstract: ZnO varistor ceramics doped with Bi_2O_3, Sb_2O_3, Co_2O_3, Cr_2O_3, and MnO_2 were prepared separately by two high-energy ball milling processes: oxide-doped and varistor ceramic powder. A comparison in the electrical and microstructural properties of the samples obtained by both methods was made. The best results on these characteristics were achieved through the high-energy ball milling varistor ceramic powder route, obtaining a nonlinear coefficient of 57 and a breakdown field of 617 V/mm at a sintering temperature of 1000 °C for 3 h. The samples synthesized by this technique show not only high density value, 95% of the theoretical density, but also a homogeneous microstructure, which compete with those obtained by the high-energy ball milling oxide-doped powder route. With the advantage that the high-energy ball milling varistor ceramic powder route can refine grain, increase the driving force of sintering, accelerate the sintering process, and reduce the sintering temperature.
Key words: varistor; ZnO; high-energy ball milling; electrical characteristic; microstructure

1 Introduction

High-energy ball milling [1,2] was developed in late 1960s for the technology preparation of materials by Benjamin of INCO milling company in United States and his collaborators. The mechanical energy created from the constant collisions among particles, balls and bowl cannot only promote the phase reaction between solid reactants but also can break down the particles to a much smaller size. Compared with normal ball-milling processes, high-energy ball milling is more efficient in strengthening the rate of reaction and modifying the particle morphology of materials [3]. High-energy ball milling of the starting powder mixture was also reported as a promising method for the preparation of varistor ceramics [2−5].

ZnO−Bi_2O_3-based varistor ceramics are semiconducting ceramic devices, which exhibit highly nonlinear voltage—current (V−I) characteristics with a high resistivity below a breakdown/threshold voltage. The nonlinear voltage−current properties are expressed by the relation $I = KV^{\alpha}$, where K is a constant and α is the nonlinear exponent. ZnO−Bi_2O_3-based varistor ceramics compositions are the most widely investigated varistor ceramics, the applications of which include voltage stabilization, transient surge suppression in electronic circuits, and electronic power systems [6]. The typical composition of ZnO−Bi_2O_3-based varistor ceramics consists of ZnO and a few mole fraction of other oxide

Foundation item: Project (BK2011243) supported by the Natural Science Foundation of Jiangsu Province, China; Project (EIPE11204) supported by the State Key Laboratory of Electrical Insulation and Power Equipment, China; Project (KF201104) supported by the State Key Laboratory of New Ceramic and Fine Processing, China; Project (KFJJ201105) supported by the Opening Project of State Key Laboratory of Electronic Thin Films and Integrated Devices, China; Project (2011-22) supported by State Key Laboratory of Inorganic Synthesis and Preparative Chemistry, China; Project (10KJD430002) supported by the Universities Natural Science Research Project of Jiangsu Province, China; Project (11JDG084) supported by the Research Foundation of Jiangsu University, China
Corresponding author: XU Dong; Tel: +86-511-88797633; E-mail: frank@ujs.edu.cn
DOI: 10.1016/S1003-6326(11)61336-8

additives, such as Sb_2O_3, Bi_2O_3, Co_2O_3, MnO_2 and Cr_2O_3. The main function of Bi_2O_3 is to promote liquid phase sintering and the formation of traps and surface states making materials with nonlinear [7]. The advantage of high-energy ball milling is that the processing of varistor ceramics is more or less the same as in the case of the standard ceramic procedure except that homogenization with low-energy milling is replaced or proceeded by high-energy dry milling. It was also reported that mechanical activation reduced the mass loss due to the volatilization of Bi_2O_3 and Sb_2O_3 [6]. High-energy ball milling will not only fracture the powder particles into smaller pieces, but also enable good mixing, thus resulting in the generation of a homogeneously mixed composite.

In this work, two different mechanical methods are used, namely, high-energy ball milling oxide-doped and varistor ceramic powder. Through comparing characteristics of ZnO varistors doped with oxide-doped and varistor ceramic powder on by high-energy ball milling, the advantage of high-energy ball milling can be described in a new perspective.

2 Experimental

ZnO–Bi_2O_3-based varistor samples with nominal compositions of 96.5 % ZnO, 0.7% Bi_2O_3, 1.0% Sb_2O_3, 0.8% Co_2O_3, 0.5% Cr_2O_3, and 0.5% MnO_2 (mole fraction, the same below if not mentioned) were mixed and homogenized in absolute ethanol media in a polyethylene bowl with zirconia balls by planetary high-energy ball milling at 100 r/min for 1 h, and the samples were labeled P0. The varistor dopant powder mixture, marked as P, which was used in reagent-grade raw materials with mole fraction of 0.7% Bi_2O_3, 1.0% Sb_2O_3, 0.8% Co_2O_3, 0.5% Cr_2O_3 and 0.5% MnO_2, and the mixtures were homogenized in absolute ethanol media in a polyethylene bowl with zirconia balls at 500 r/min for 5 h by planetary high-energy ball milling. Then the powder samples (3.5% P+96.5% ZnO) were ball milled at 500 r/min for 0 h (instead for 1 h at 100 r/min), at 500 r/min for 1 h, at 500 r/min for 5 h, at 500 r/min for 10 h, and were marked as P1, P2, P3 and P4, respectively. The slurry was dried at 70 °C for 24 h, pulverized by an agate mortar/pestle after 2% (mass fraction) polyvinyl alcohol (PVA) binder had been added, and granulated by sieving through a sieve of 0.15 mm to produce the starting power. The powders were then dried and pressed into discs with a diameter of 12 mm and a thickness of 2.0 mm. The pressed disks were sintered in air at 1000, 1100, 1200 °C (2 h dwell time), and at a heating rate of 5 °C/min, cooled in the furnace, and then marked with the letters A, B and C, respectively, for identification.

ZnO–Bi_2O_3-based varistor samples with nominal compositions of 96.5% ZnO, 0.7% Bi_2O_3, 1.0% Sb_2O_3, 0.8% Co_2O_3, 0.5% Cr_2O_3, and 0.5% MnO_2 were used. Reagent-grade raw materials were mixed and homogenized in absolute ethanol media in a polyethylene bowl with zirconia balls by planetary high-energy ball milling at 500 r/min for 0, 1, 3, 5 and 10 h, and the samples were labeled as D0, D1, D2, D3 and D4, respectively. The mass ratio of balls to the mixed powder was 20:l. The slurry was dried at 70 °C for 24 h after selecting by a sieve of 0.063 mm, pulverized by an agate mortar/pestle after 2% (mass fraction) polyvinyl alcohol (PVA) binder was added, and then granulated by a 0.15 mm sieve to produce the starting power. The powders were then dried and pressed into discs with a diameter of 12 mm and a thickness of 2.0 mm. The samples were put into VMK1400 high temperature experimental electric furnace which was made in Germany. The pressed disks were sintered in air at 1100 °C for 2 h dwell time, and then with a heating rate of 5 °C/min [7−10], cooled in the furnace. The pressed disks were sintered in air at 900, 1000, 1100 °C for 2 h dwell time, with a heating rate of 5 °C/min and then cooled in the furnace, and then marked with the letters A, B and C, respectively, for identification.

The relatively density (D) is defined by the percentage of actual density and theoretical density [11−13]. For the characterization of DC current—voltage, the silver paste was coated on both faces of samples and the silver electrodes were formed by heating at 600 °C for 10 min. The electrodes were 5 mm in diameter. Using varistor DC parameters device (CJ1001, Chongjie Electronics Co., Ltd., Changzhou) to measure the voltage V_{1mA} and $V_{0.1mA}$ under 1.0 mA and 0.1 mA, potential gradient $V_T=V_{1mA}/d$ (d is thickness), nonlinear coefficient α ($\alpha=1/\lg(V_{1.0mA}/V_{0.1mA})$) at 0.1−1.0 mA. The current density (J_L) of drain current (I_L) is measured by the equation $J_L=I_L/S$, where S is the area of awaiting measuring samples' extremity electrode [11,14]. The crystalline phases were identified by the X-ray diffractometer (XRD, Rigaku D/max 2200, Japan) using a Cu K_α radiation. A scanning electron microscope (SEM, FEI QUANTA 400) was used to examine the surface microstructure.

3 Results and discussion

3.1 High-energy ball milling oxide-doped

The XRD spectra of samples which were sintered at 1000 and 1100 °C respectively are given in Fig. 1. Figure 1 shows that the XRD diffraction peak of ZnO−Bi_2O_3-based varistor ceramics does not change largely, which proves that high-energy ball milling does not make varistor ceramics generate a new phase. We can also see that all samples contain the basic

components of varistor ceramics, and they are ZnO phase, spinel phase $Zn_7Sb_2O_{12}$, a small amount of Bi-rich phase and pyrochlore phase $Bi_3Zn_2Sb_3O_{14}$ [15,16]. When the sintering temperature is high, such as 1100 °C, the Bi-rich phase in varistor ceramics will decrease gradually, which indicates that a part of Bi-rich phase volatilizes with an increase of sintering temperature.

Figure 2 shows the SEM images of varistors sintered at 1100 °C and then ball mined for zinc, milling time is 0, 1, 5, 10 h, respectively. The 5 h-milling sample has the smallest grains, and its grain interstice phase (spinel phase) and grain boundary phase (Bi-rich phase) are more refined.

In order to study the impact of high-energy ball milling oxide-doped powder on ZnO−Bi_2O_3-based varistor ceramics, the electrical properties and densities of samples by different milling processes at different sintering temperatures were tested.

From Fig. 3, we can see that the electrical property and density of the sample reach up to a high-point when the balling milling time is 5 h and the sintering temperature is 1100 °C. With an increase in sintering temperature to 1100 °C, the voltage gradient, nonlinear coefficient as well as the density of varistor ceramics will

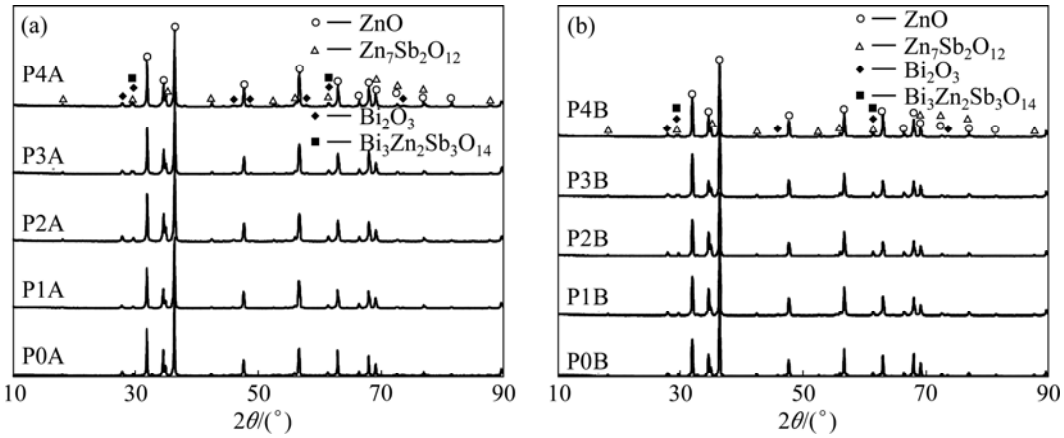

Fig. 1 XRD patterns of varistors sintered at different temperatures: (a) 1000 °C, (b) 1100 °C

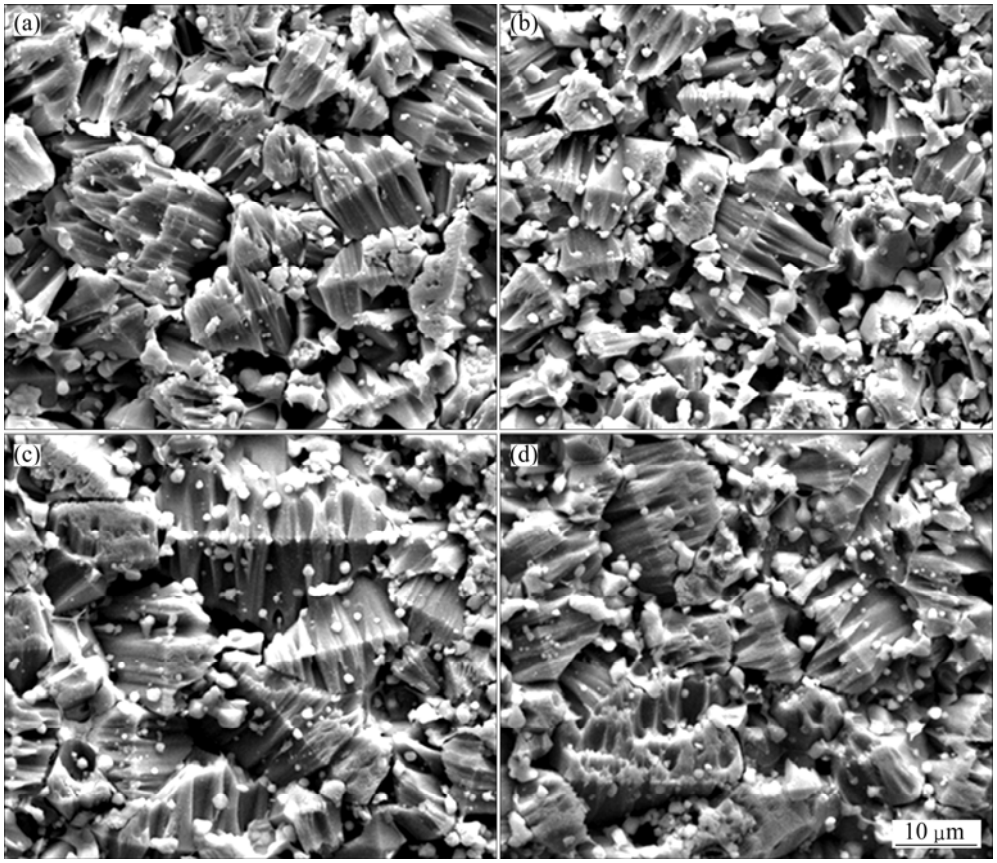

Fig. 2 SEM images of varistors sintered at 1100 °C and milled for different time: (a) 0 h; (b) 1 h; (c) 5 h; (d) 10 h

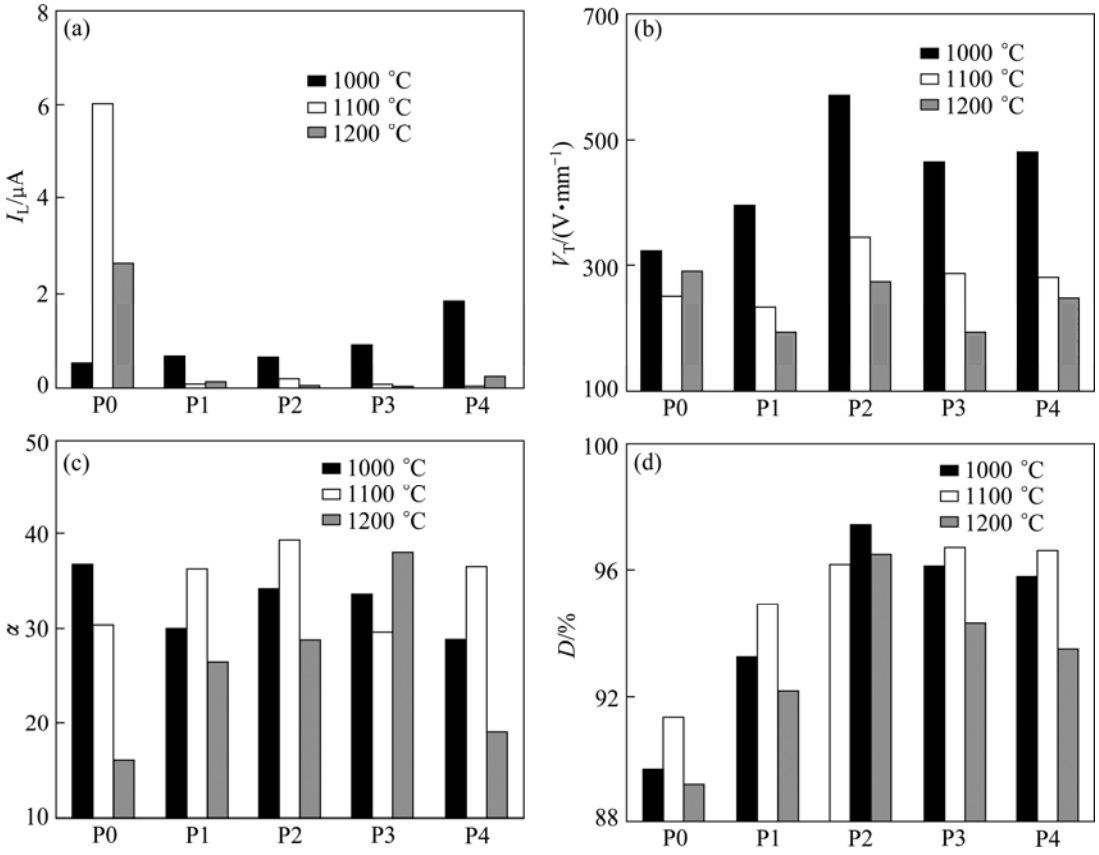

Fig. 3 Electrical properties and density of varistors at different sintering temperatures: (a) I_L; (b) V_T; (c) α; (d) D

decrease gradually, but the leakage current will increase. The potential gradient (V_T) of ZnO−Bi_2O_3-based varistor ceramics can be calculated by the following equation:

$$V_T=N_{gb}V_{gb}/d \quad (1)$$

where N_{gb} is the number of grain boundary in a unit length, V_{gb} means the breakdown voltage of a single grain boundary, and d is the average size of grain. When the grain is fully semiconducted, we generally consider that V_{gb} is a constant. Thus, V_T is inversely proportional to the grain size. With the increase of sintering temperature, the grain grows up gradually. So V_{gb} decreases monotonically. Meanwhile, the increase of sintering temperature is conducive to the liquid phase recrystal, which may promote the grain growth and even distribution of crystal varistor ceramics, and make the resistance in the internal grain decrease to reduce the potential gradient of varistor ceramics. In addition, with the increase of sintering temperature, ZnO−Bi_2O_3-based varistor ceramics contraction is intensified, so its porosity is reduced, and its internal structure is more compact.

Therefore, the potential gradient of varistor ceramics is reduced, while the nonlinear is increased. However, if the sintering temperature is too high, the ingredients with low melting point in varistor ceramics such as Bi_2O_3 may be apt to volatilize, resulting in the reduction of the grain boundary barrier, and the damage of some grains' boundary structure (the depletion layer is destroyed). So, the grain boundary layer will become thinner and thinner, or even disappear, leading to the high dispersion of potential gradient of varistor ceramics and sharp decline of nonlinear coefficient. Besides, other electrical properties may also deteriorate.

When the sintering temperature is from 500 to 1050 °C, ZnO−Bi_2O_3-based varistor ceramics have the following reactions in the sintering process:

$$Sb_2O_3(s)+O_2 \longrightarrow Sb_2O_5\ (l) \quad (527\ °C) \quad (2)$$

$$Sb_2O_5(l)+ZnO(s) \longrightarrow ZnSb_2O_6(s) \quad (700-800\ °C) \quad (3)$$

$$ZnSb_2O_6(s)+6ZnO(s) \longrightarrow Zn_7Sb_2O_{12}(s) \quad (>800\ °C) \quad (4)$$

$$3ZnSb_2O_6(s)+3Bi_2O_3(s)+ZnO(s) \longrightarrow 2Zn_2Bi_3Sb_3O_{14}(s) \quad (700\ °C<t<900\ °C) \quad (5)$$

$$2Zn_2Bi_3Sb_3O_{14}(s)+17ZnO(s) \longrightarrow 3Zn_7Sb_2O_{12}(s)+3Bi_2O_3(l) \quad (950-1050\ °C) \quad (6)$$

$$Zn_7Sb_2O_{12}(s)+Bi_2O_3(l) \rightarrow Bi_2O_3(Sb,Zn)(l) \quad (1050\ °C) \quad (7)$$

At the first stage of sintering, the spinel phase will form from Eqs. (2)−(7), and then the pyrochlore phase. For these reactions need to consume Bi_2O_3, the volatilization of Bi_2O_3 will slow down. Equation (6)

shows that the reaction between pyrochlore phase and ZnO will generate Bi_2O_3 liquid phase, which will melt ZnO nearby and generate Bi-rich liquid phase, while the capillary force produced by Bi-rich liquid will lead to the aggregation and concatenation of the second-phase. Although Eq. (6) causes the reduction of pyrochlore phase and the increase of spinel phase, this kind of concatenate organization still exists at the end of the sintering. The grains of this concatenate second-phase are coarse with uneven distribution. At the same time, due to the formation of Bi-rich liquid, the volatilization begins. From Eq. (6), it can be seen that when the temperature rises to 1000 °C, the volatilization of ceramic varistor Bi_2O_3 exacerbates. Although the emergence of Bi-rich liquid phase is temporary, it still enhances the densification process of ceramic varistor. The emergence of the second-phases such as pyrochlore phase and spinel phase increases the diffusion distance between zinc oxide grains, thus generating a hinder effect on the densification.

The nonlinear coefficient of the 5 h-milling sample's potential gradient is high and the leakage current is low. The density of voltage dependent resistor rises with the increase of milling time, mainly due to the high energy mechanical milling refining grain size, which makes the lattice distortion increase, significantly improves the sintering driving force as well as the sintering kinetics factor, and shortens the reaction-diffusion distance. Liquid phase generated by sintering makes the contact area of reaction increase, accelerates the mass transfer rate and promotes the inner-phase response. With the prolongation of milling time, the potential gradient of the sample with the milling time of 10 h increases slowly, and nonlinear coefficient and leakage current all begin to deteriorate. High-energy ball milling means that there is an agglomerate dynamic process accompanied by the crush process of a powder. Under the impact of crushing forces and friction, the grain size of powder decreases rapidly, and may achieve the dynamic equilibrium with prolonging the milling time; then the prolonging milling time will no longer play the role in grain refinement, but it may introduce some of zirconia impurities, resulting in the deterioration of electrical properties. Therefore, the 5 h-high-energy ball milling can be used to prepare the raw material powder with higher purity and smaller grain size.

3.2 High-energy ball milling varistor ceramic

The XRD spectra of samples which were sintered at 1000 °C, 1100 °C respectively are given in Fig. 4. Figure 4 shows that the XRD diffraction peak of varistor ceramic does not change greatly; however, it also proves that high-energy ball milling does not make varistor ceramics generate a new phase. We can also see that all samples contain the basic components of $ZnO-Bi_2O_3$-based varistor ceramics, which are ZnO phase, spinel phase $Zn_7Sb_2O_{12}$, a small amount of Bi-rich phase and pyrochlore phase $Bi_3Zn_2Sb_3O_{14}$ [17−19].

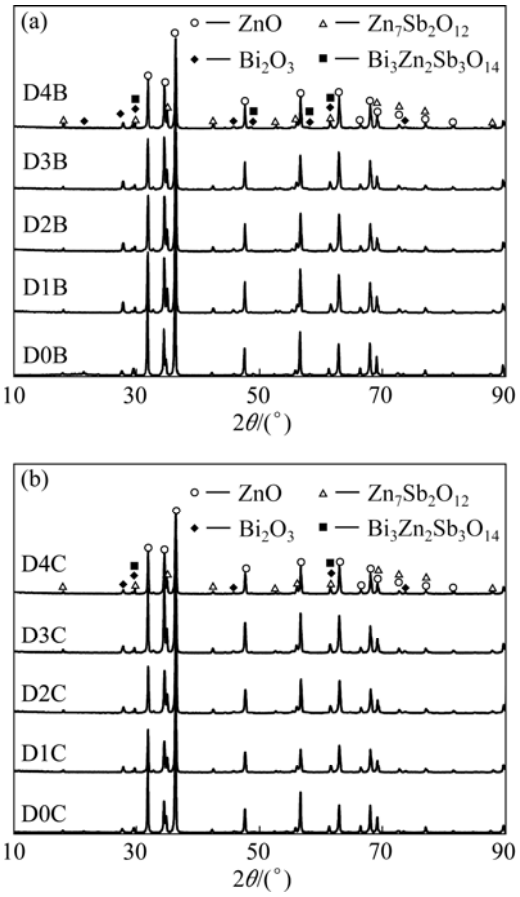

Fig. 4 XRD patterns of varistors sintered at different temperatures: (a) 1000 °C, (b) 1100 °C

Figure 5 shows that SEM images of the high-energy ball milling varistor ceramic powders with the milling time of 0, 1, 3, 5, 10 h (samples labeled as D0B, D1B, D2B, D3B, D4B) respectively and the sintering temperature of 1000 °C. As shown in Fig. 5, with an increase in the milling time, the varistor ceramics grain size becomes small, and the grain size of varistor ceramic is the smallest with 10 h-milling.

In order to study the influence of high-energy ball milling varistor ceramic powder on $ZnO-Bi_2O_3$-based varistor ceramics, we measured the electrical properties and density of samples under different sintering temperatures and milling times.

As shown in Fig. 6, the 3h-milling sample owns the best properties when sintered at 1000 °C. The leakage current of the sample sintered at 900 °C is too heavy which exceeds industrial regulation (50 μA). Compared with those samples sintered at 1000 °C and

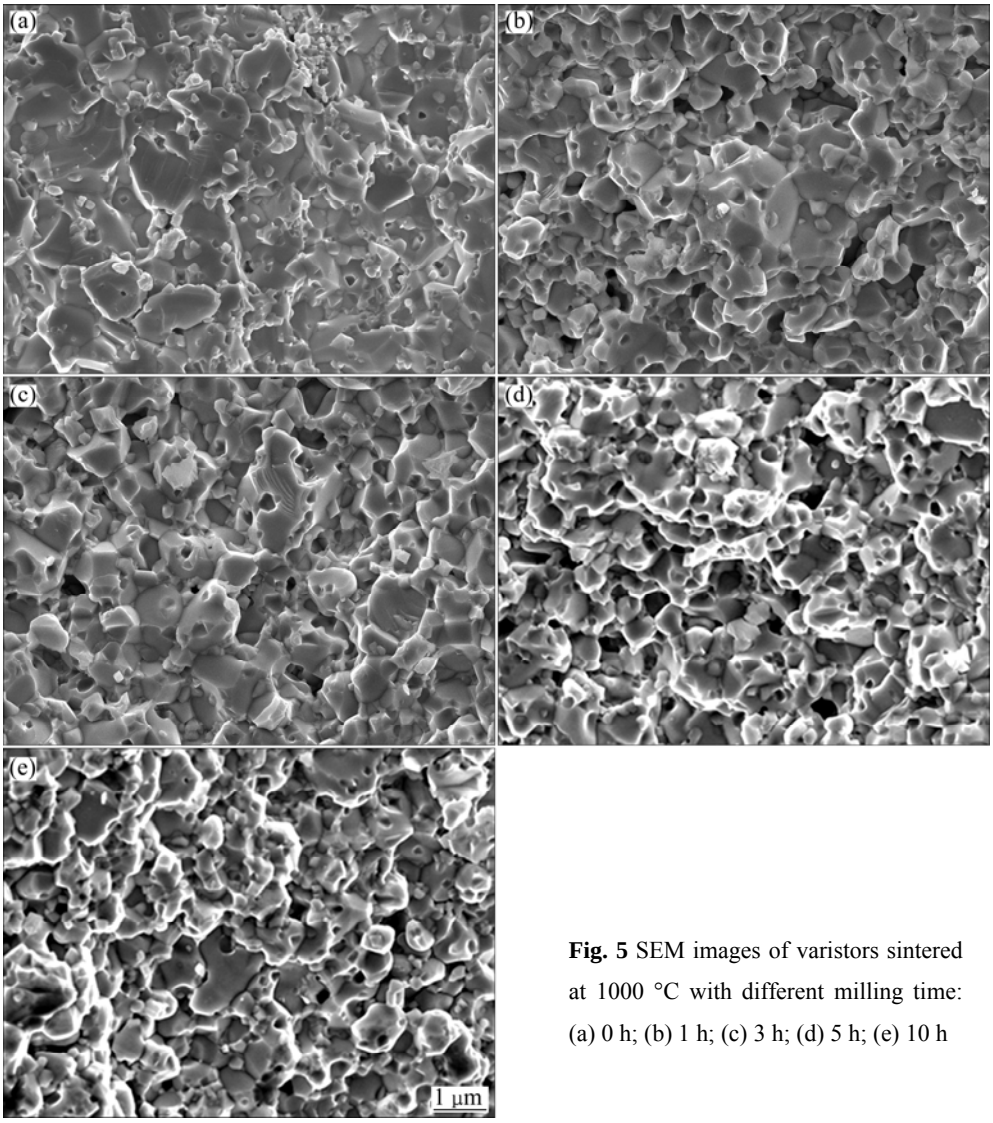

Fig. 5 SEM images of varistors sintered at 1000 °C with different milling time: (a) 0 h; (b) 1 h; (c) 3 h; (d) 5 h; (e) 10 h

1100 °C, it is apparent that the former has better electrical properties, such as low leakage current, high nonlinear coefficient, high potential gradient, and good density. In the voltage dependent resistor, $E_s=nV_b$, where E_s is the breakdown field strength, n is the Schottky barrier in the direction of current conduction in per unit length and V_b is the voltage drop of each barrier, usually 2−4 V. Therefore, E_s depends on the values of n. With the climbing of sintering temperature, the grain grows up gradually to a contrast, and n decreases. From the equation $E_s=nV_b$, it can be seen that potential gradient will decline.

The sample sintered at 1000 °C has better properties than at 1100 °C for the high-energy ball milling can refine the grains, while the refined grains have a strong activity on their surface. The addition of the sintering driving force can shorten the atom diffusion distance and improve the solubility of grains in the liquid phase for the purpose of accelerating the sintering process and reducing the sintering temperature. The optimum sintering temperature of 1000 °C is 100 °C lower than the normal solid state sintering temperature of 1100 °C which can effectively save the productive cost.

The 3h-milling sample has the highest nonlinear coefficient, higher potential gradient and density, and lower leakage current. However, the 5 h-milling grain has the smallest size probably because that high energy ball milling media of zirconia lead to the pollution on powders, which will affect the electrical properties of ZnO−Bi_2O_3-based varistor ceramics. Moreover, overlong milling time may lead to deterioration of electrical properties of varistor ceramics.

3.3 Comparison of electrical properties of samples formulated by two different milling processes

The relationships between electrical properties and density of samples P and D sintered at 1000 °C are shown from Fig. 7. It can be seen that those samples prepared by high-energy ball milling varistor ceramic powder are better than oxide-doped.

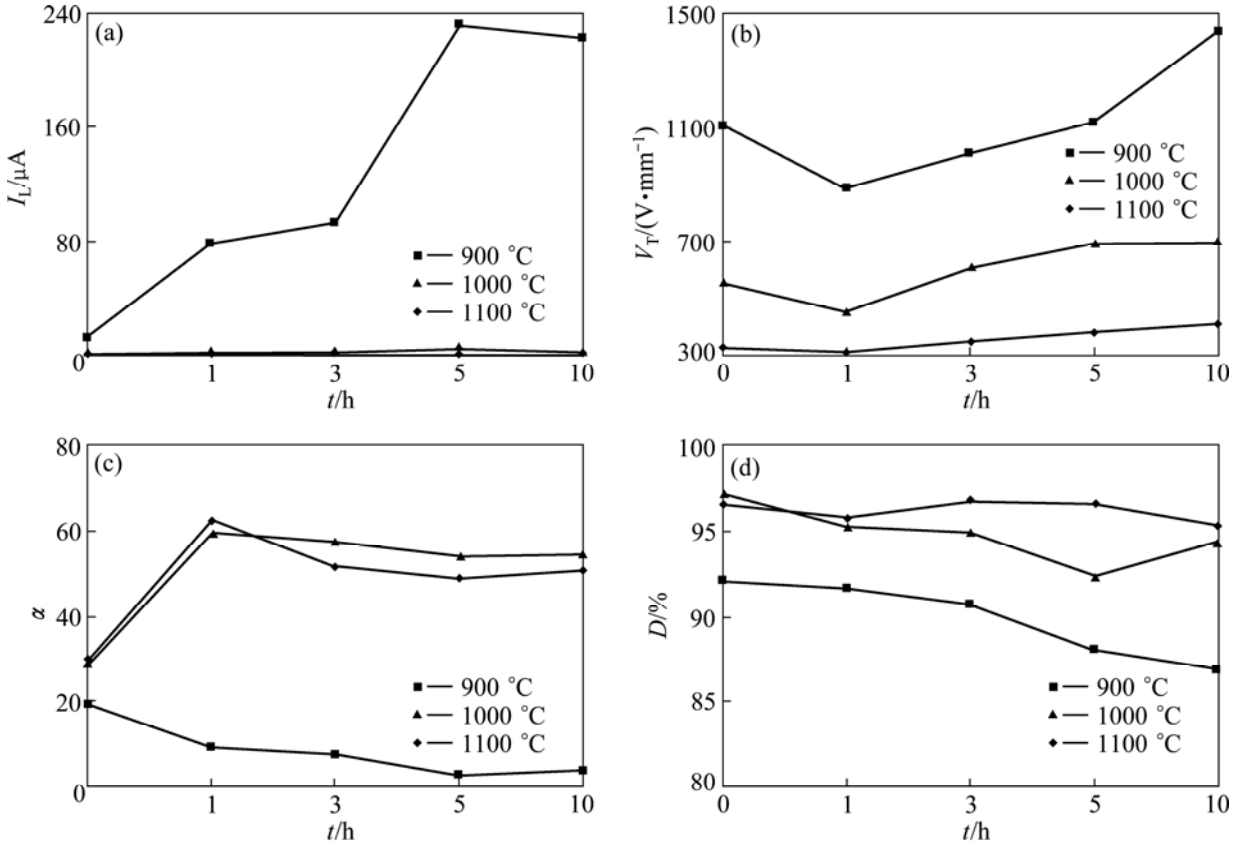

Fig. 6 Electrical properties and density of varistors sintered at different temperatures for different time: (a) I_L; (b) V_T; (c) α; (d) D

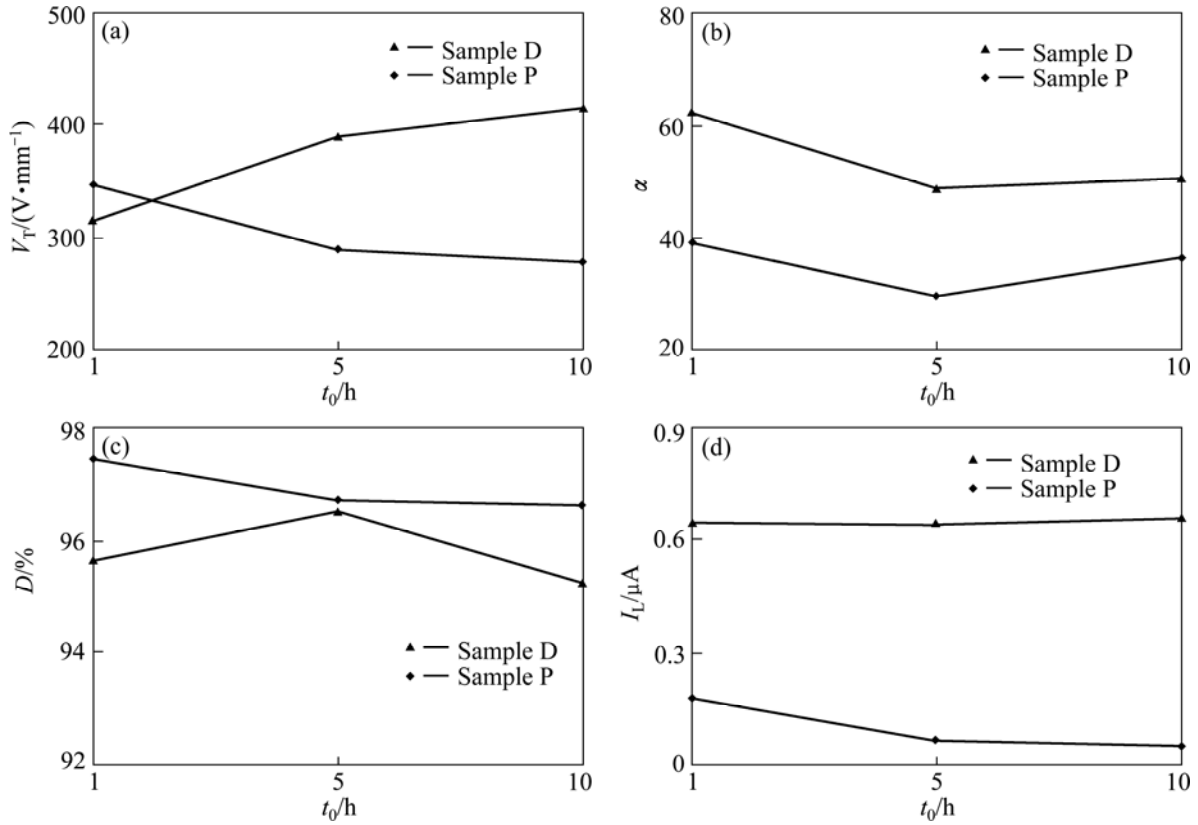

Fig. 7 Electrical properties and density of samples prepared by two different milling processes and then sintered at 1000 °C for different time: (a) V_T; (b) α; (c) D; (d) I_L

The potential gradient, nonlinear coefficient and relative density are higher, the leakage current is lower than 50 μA. This indicates that high-energy ball milling varistor ceramic powder has improved the properties. High-energy ball milling will not only fracture the powder particles into fine pieces, but also enable the powder mix well, thus resulting in the generation of a homogeneously mixed composite.

4 Conclusions

1) ZnO−Bi_2O_3-based varistor ceramics were prepared separately by two high-energy ball milling processes: oxide-doped and varistor ceramic powder. Varistor ceramics were prepared by high-energy ball milling oxide-doped powder and sintered at 1100 °C for 5 h to obtain the best comprehensive electrical properties, the potential gradient of 347 V/mm, nonlinear coefficient of 39.

2) The best results of these characteristics were achieved through the high-energy ball milling varistor ceramic powder route, a nonlinear coefficient of 57 and a breakdown field of 617 V/mm at a sintering temperature of 1000 °C for 3 h. The samples synthesized by this technique show not only high density values, 95% of the theoretical density, but also a homogeneous microstructure, which compete with those obtained by the high-energy ball milling oxide-doped powder route.

3) The high-energy ball milling varistor ceramic powder route can refine grain, increase the driving force of sintering, accelerate the sintering process, and reduce the sintering temperature.

References

[1] LAO Y W, KUO S T, TUAN W H. Influence of ball milling on the sintering behaviour of ZnO powder [J]. Ceramics International, 2009, 35(3): 1317−1320.

[2] PARK K, KIM J G, LEE K J, CHO W S, HWANG W S. Electrical properties and microstructure of Y-doped $BaTiO_3$ ceramics prepared by high-energy ball-milling [J]. Ceramics International, 2008, 34(7): 1573−1577.

[3] AGUILAR-MARTINEZ J A, HERNANDEZ M B, PECH-CANUL M I, GLOT A B, CASTILLO-TORRES J. A comparative study between the mixed-oxide and high-energy milling planetary method on electrical and microstructural properties for a SnO_2-based ceramic system [J]. Journal of Materials Processing Technology, 2009, 209(1): 318−323.

[4] BERNIK S, BRANKOVIC G, RUSTJA S, ZUNIC M, PODLOGAR M, BRANKOVIC Z. Microstructural and compositional aspects of ZnO-based varistor ceramics prepared by direct mixing of the constituent phases and high-energy milling [J]. Ceramics International, 2008, 34(6): 1495−1502.

[5] BRANKOVIC Z, BRANKOVIC G, BERNIK S, ZUNIC M. ZnO varistors with reduced amount of additives prepared by direct mixing of constituent phases [J]. Journal of the European Ceramic Society, 2007, 27(2−3): 1101−1104.

[6] ASHRAF M A, BHUIYAN A H, HAKIM M A, HOSSAIN M T. Microstructure and electrical properties of Sm_2O_3 doped Bi_2O_3-based ZnO varistor ceramics [J]. Materials Science and Engineering B, 2011, 176(11): 855−860.

[7] XU Dong, SHI Li-yi, WU Zhen-hong, ZHONG Qing-dong, WU Xin-xin. Microstructure and electrical properties of ZnO-Bi_2O_3-based varistor ceramics by different sintering processes [J]. Journal of the European Ceramic Society, 2009, 29(9): 1789−1794.

[8] WU Zhen-hong, FANG Jian-hui, XU Dong, ZHONG Qing-dong, SHI Li-yi. Effect of SiO_2 addition on the microstructure and electrical properties of ZnO-based varistors [J]. International Journal of Minerals, Metallurgy and Materials, 2010, 17(1): 86−91.

[9] XU Dong, SHI Xiao-feng, CHENG Xiao-nong, YANG Juan, FAN Yue-e, YUAN Hong-ming, SHI Li-yi. Microstructure and Electrical Properties of Lu_2O_3-doped ZnO-Bi_2O_3-based varistor ceramics [J]. Transactions of Nonferrous Metals Society of China, 2010, 20(12): 2303−2308.

[10] XU Dong, CHENG Xiao-nong, YAN Xue-hua, XU Hong-xing, SHI Li-yi. Sintering process as relevant parameter for Bi_2O_3 vaporization from ZnO-Bi_2O_3-based varistor ceramics [J]. Transactions of Nonferrous Metals Society of China, 2009, 19(6): 1526−1532.

[11] XU Dong, CHENG Xiao-nong, YUAN Hong-ming, YANG Juan, LIN Yuan-hua. Microstructure and electrical properties of $Y(NO_3)_3{\cdot}6H_2O$-doped ZnO-Bi_2O_3-based varistor ceramics [J]. Journal of Alloys and Compounds, 2011, 509(38): 9312−9317.

[12] XU Dong, ZHANG Chen, HENG Xiao-nong, FAN Yue-e, YANG Tao, YUAN Hong-ming. Dielectric properties of Zn-doped CCTO ceramics by sol-gel method [J]. Advanced Materials Research, 2011, 197−198: 302−305.

[13] XU Dong, CHENG Xiao-nong, WANG Ming-song, SHI Li-yi. Microstructure and electrical properties of La_2O_3-doped ZnO-Bi_2O_3-based varistor ceramics [J]. Advanced Materials Research, 2009, 79−82: 2007−2010.

[14] XU Dong, CHENG Xiao-nong, ZHAO Guo-ping, YANG Juan, SHI Li-yi. Microstructure and electrical properties of Sc_2O_3-doped ZnO-Bi_2O_3-based varistor ceramics [J]. Ceramics International, 2011, 37(3): 701−706.

[15] ASHRAF M A, BHUIYAN A H, HAKIM M A, HOSSAIN M T. Microstructure and electrical properties of Ho_2O_3 doped Bi_2O_3-based ZnO varistor ceramics [J]. Physica B, 2010, 405(17): 3770−3774.

[16] ÖZGÜR ÖZER İ, SUVACI E, BERNIK S. Microstructure-property relationship in textured ZnO-based varistors [J]. Acta Materialia, 2010, 58(12): 4126−4136.

[17] PEITEADO M, IGLESIAS Y, CABALLERO A C. Sodium impurities in ZnO-Bi_2O_3-Sb_2O_3 based varistors [J]. Ceramics International, 2011, 37(3): 819−824.

[18] SAVARY E, MARINEL S, GASCOIN F, KINEMUCHI Y, PANSIOT J, RETOUX R. Peculiar effects of microwave sintering on ZnO based varistors properties [J]. Journal of Alloys and Compounds, 2011, 509(21): 6163−6169.

[19] SHAHRAKI M M, SHOJAEE S A, SANI M, NEMATI A, SAFAEE I. Two-step sintering of ZnO varistors [J]. Solid State Ionics, 2011, 190(1): 99−105.

高能球磨掺杂氧化物粉体和压敏陶瓷粉体对氧化锌压敏陶瓷性能的影响

徐 东[1,2,3], 唐冬梅[1,4], 焦 雷[1], 袁宏明[5], 赵国平[1], 程晓农[1,4]

1. 江苏大学 材料科学与工程学院, 镇江 212013;
2. 中国科学院 半导体研究所，半导体材料科学重点实验室, 北京 100083;
3. 西安交通大学 电力设备与电气绝缘国家重点实验室, 西安 710049;
4. 常州江苏大学工程技术研究院, 常州 213000;
5. 吉林大学 化学学院, 无机合成与制备化学国家重点实验室, 长春 130012

摘 要：采用高能球磨掺杂氧化物粉体和压敏陶瓷粉体 2 种不同制备技术制备 $ZnO-Bi_2O_3$ 压敏陶瓷，通过扫描电镜和 X-射线衍射对其显微组织和相成分进行分析，探讨不同高能球磨制备技术对氧化锌压敏陶瓷电性能和显微组织的影响。结果表明：压敏陶瓷粉体高能球磨是制备高性能氧化锌压敏陶瓷的一种优异的技术，在 1000 °C 下烧结 3 h，压敏陶瓷的电位梯度为 617 V/mm，非线性系数为 57；压敏陶瓷的致密度高达 95%，显微组织均匀、致密；高能球磨压敏陶瓷粉体可细化晶粒，增强烧结驱动力，加速烧结过程，降低烧结温度。

关键词：压敏电阻；氧化锌；高能球磨；电性能；显微组织

(Edited by LI Xiang-qun)